transients were accumulated with a delay time of 50 ms. The signal-to-noise ratio was improved by apodization of the free induction decay. The residual proton peak of dichloromethane-d_2 was used as a secondary reference (5.32 ppm). Intense diamagnetic resonances arising from $[(PPh_3)_2N]CN$ and 4-MeIm were suppressed with a Super WEFT pulse sequence.[41] This resulted in inversion of some slowly relaxing diamagnetic resonances. The delay time τ between the 180° pulse and the 90° pulse was typically greater than 50 ms, and the effect on the intensity of the paramagnetic resonances was negligible. Figure 6 was obtained with the CAChe system of Tektronix Inc.

Acknowledgment. We thank the National Institutes of Health (Grant GM-26226) for support and Dr. Linda M. Hirschy of Tektronix, Inc. for generating Figure 6 using the CAChe molecular modeling program.

(41) Inubushi, T.; Becker, E. D. *J. Magn. Reson.* **1983**, *51*, 128-133.

Registry No. $[Ph_2SMe]BF_4$, 10504-60-6; (*N*-MeTMP)$Fe^{II}Cl$, 128901-96-2; (Thian$^+$)$SbCl_6$, 76598-11-3; [(*N*-MeTPP)$Fe^{III}Cl$]-$[SbCl_6]$·1.5(toluene), 128901-98-4; *N*-MeTTP$Fe^{II}Cl$, 95675-71-1; (*N*-MeTTP)$Fe^{III}(CN)_2$, 128901-99-5; $[(N\text{-MeTTP})Fe^{III}(5\text{-MeIm})_2]^{2+}$, 128901-95-1; $[(N\text{-MeTMP})Fe^{III}Im_2]^{2+}$, 128901-94-0; [(*N*-MeTMP)-$Fe^{III}Cl]^+$, 128902-00-1; $[(N\text{-MeTTP})Fe^{III}Cl][SbCl_6]$, 128902-01-2; *N*-methyltetramesitylporphyrin, 128901-93-9; tetramesitylporphyrin, 56396-12-4; iodomethane, 74-88-4; diphenyl sulfide, 139-66-2; silver tetrafluoroborate, 14104-20-2; thianthrene, 92-85-3; antimony pentachloride, 7647-18-9.

Supplementary Material Available: Tables of atomic coordinates, bond distances, bond angles, anisotropic thermal parameters, hydrogen atom positions, and crystal refinement data for $[(N\text{-MeTTP})FeCl]SbCl_6$·1.5(toluene) (8 pages); listings of observed and calculated structure factors (29 pages). Ordering information is given on any current masthead page.

Reactions Involving Chelate Ring Opening or Metal Ion Relocation in the Formation of Luminescent Complexes Containing both Gold and Iridium

Alan L. Balch,* Vincent J. Catalano, Bruce C. Noll, and Marilyn M. Olmstead

Contribution from the Department of Chemistry, University of California, Davis, California 95616. *Received March 19, 1990*

Abstract: Treatment of $Ir(CO)_2Cl$(*p*-toluidine) with 2 equiv of dpmp (bis(diphenylphosphinomethyl)phenylphosphine) and ammonium hexafluorophosphate yields ivory $[Ir(dpmp)_2CO][PF_6]$, **5**, which an X-ray crystal structure shows to have a five-coordinate geometry with one six-membered and one four-membered chelate ring. This structure is compared with that of $[Ir(dpma)_2CO][PF_6]$, **3** (dpma is bis(diphenylphosphinomethyl)phenylarsine), which is trigonal-bipyramidal with two six-membered chelate rings that span axial and equatorial coordination sites. Addition of 3 equivs of Me_2SAuCl to **5** results in the formation of orange $[Ir(CO)ClAu(AuCl)_2(\mu\text{-dpmp})_2][PF_6]$, **6**, which has a planar $Ir(CO)Cl(P)_2$ unit connected to the trans, terminal phosphorus atoms of the dpmp ligands, an Au(I) ion bound to the two internal phosphorus atoms, and AuCl moieties attached to the remaining two terminal phosphorus atoms of the dpmp ligands. Complex **6** has a strong absorption at 454 nm and photoemissions at 568 and 660 nm. Treatment of **6** with KCN or **5** with KCN and Me_2SAuCl results in the formation of centrosymmetric $[Au_2Ir(CN)_2(\mu\text{-dpmp})_2][PF_6]$, **7**, with a linear Au-Ir-Au chain. The conversion of **6** to **7** results not only in loss of a gold ion but also extensive rearrangement at the core to go from a T-shaped Au_2AuIr unit to a linear AuIrAu section. Complex **7** is intensely magenta (λ_{max}(absorption) = 578 nm) with photoemission at 612 and 782 nm.

Introduction

The metallomacrocycle **1** and its rhodium analogue have been useful starting materials for the rational preparation of a wide variety of heterotrinuclear complexes via reaction 1.[1] Both

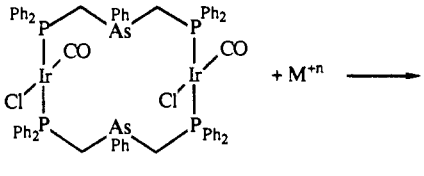

1

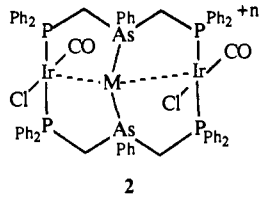

2 (1)

transition-metal ions (including Cu(I), Ag(I), Au(I), Pd(II), Rh(I), and Ir(I))[2] and main-group ions (including Tl(I), In(I), Sn(II), and Pb(II))[3] have been incorporated into the framework provided by **1**. We have also recently discovered another route to the formation of mixed-metal trinuclear species. This involves the opening of six-membered chelate rings in the complex $[Ir(dpma)_2(CO)][PF_6]$, **3** (dpma is bis(diphenylphosphinomethyl)-phenylarsine, the same ligand seen in eq 1).[4] In this process, reaction 2, there is considerably more bond breaking than necessary in reaction 1. In fact, only the Ir-CO bond is retained (as is the 2:1:1 dpma:Ir:CO stoichiometry). Eight metal-ligand bonds must break in the process, while seven new metal-ligand bonds as well as two gold-iridium bonds are formed. This opening of the six-membered chelate ring in **3** was particularly surprising,

(1) Balch, A. L. *Pure Appl. Chem.* **1988**, *60*, 555.

(2) (a) Balch, A. L.; Fossett, L. A.; Olmstead, M. M.; Oram, D. E.; Reedy, P. E., Jr. *J. Am. Chem. Soc.* **1985**, *107*, 5272. (b) Balch, A. L.; Fossett, L. A.; Olmstead, M. M.; Reedy, P. E., Jr. *Organometallics* **1986**, *5*, 1929. (c) Balch, A. L.; Olmstead, M. M.; Neve, F.; Ghedini, M. *New. J. Chem.* **1988**, *12*, 529, and references in each.

(3) (a) Balch, A. L.; Nagle, J. K.; Olmstead, M. M.; Reedy, P. E., Jr. *J. Am. Chem. Soc.* **1987**, *109*, 4123. (b) Balch, A. L.; Olmstead, M. M.; Oram, D. E.; Reedy, P. E., Jr.; Reimer, S. H. *J. Am. Chem. Soc.* **1989**, *111*, 4021.

(4) Balch, A. L.; Catalano, V. J.; Olmstead, M. M. *J. Am. Chem. Soc.* **1990**, *112*, 2010.

0002-7863/90/1512-7558$02.50/0

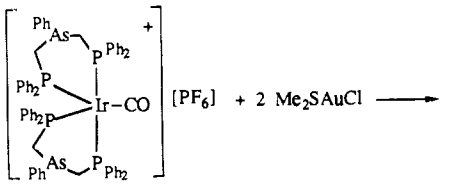

3

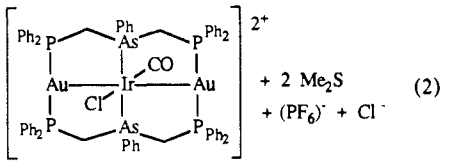

4 (2)

since previous work had shown that other related chelate rings derived from dpmp (bis(diphenylphosphinomethyl)phenylphosphine, the phosphine analogue of dpma) could bind an additional metal ion through the central, uncoordinated phosphorus atom but did not undergo ring opening (eq 3).[5]

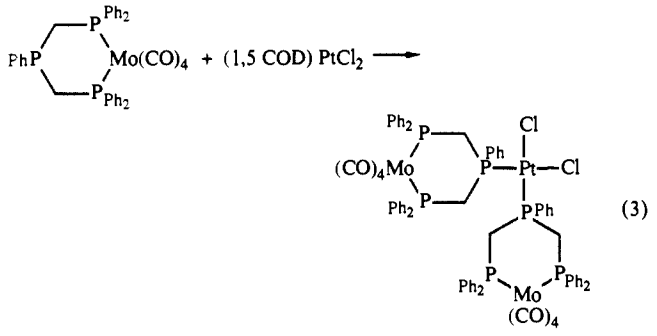

(3)

We are actively investigating the behavior of chelated complexes similar to **3** and are exploring the reactivity of **3** itself toward a range of metal ions other than gold. Here we describe the rather remarkable results of turning our attention to the dpmp analogue of **3** and exploring its reactivity toward gold(I) complexes.

Results

Synthetic Studies. The reaction chemistry described here is summarized in Scheme I. Treatment of $Ir(CO)_2Cl(p\text{-tolNH}_2)$ (p-tolNH$_2$ is p-toluidine) with 2 equiv of dpmp followed by the additional of ammonium hexafluorophosphate produces yellow crystals of $[Ir(CO)(dpmp)_2][PF_6]$, **5**. These have good solubility in dichloromethane, acetone, and acetonitrile but are essentially insoluble in ethyl ether and hydrocarbons. Under identical conditions, but using dpma in place of its triphosphine analogue, ivory $[Ir(CO)(dpma)_2][PF_6]$, **3**, is formed. Although both **3** and **5** have similar stoichiometries and solubilities, their structures are clearly different. There are differences in their infrared spectra (ν(CO) for **5**, 1946 cm^{-1}; 1971 for **3** in mineral ion mulls), and their $^{31}P\{^1H\}$ NMR spectra are notably different. These structural differences are documented in the next section.

Addition of 3 equiv of colorless Me_2SAuCl to yellow $[Ir(CO)(dpmp)_2][PF_6]$ in dichloromethane at 23 °C produces an intense red-orange solution from which orange crystals of $[Ir(CO)ClAu(AuCl)_2(\mu\text{-dpmp})_2][PF_6]$, **6**, are formed in 85% yield after the addition of diethyl ether. The infrared spectrum (ν(CO) 1973 cm^{-1} in mineral oil mull) is consistent with the presence of an Ir(I)CO unit within the complex.

We attempted to form the hypothetical $[Au_2Ir(CO)Cl(\mu\text{-dpmp})_2]^+$ with an Au–Au–Ir trinuclear fragment by selective removal of one gold ion from **6**. For this we chose reaction with cyanide ion under the expectation that a gold ion would be removed to form the very stable $Au(CN)_2^-$. Treatment of the orange complex **6** in dichloromethane with potassium cyanide in methanol results in a striking change in the color to deep magenta. Addition of methanolic ammonium hexafluorophosphate and concentration yields deep purple crystals of $[Ir(CN)_2Au_2(\mu\text{-dpmp})_2][PF_6]$, **7**, in 70% yield. These have good solubility in dichloromethane, acetone, and acetonitrile and moderate solubility in methanol but are essentially insoluble in ethyl ether and hydrocarbons. The infrared spectrum reveals ν(CN) at 2128 cm^{-1} (in mineral oil mull) and no features in the region 2100–1650 cm^{-1}. Thus no carbon monoxide ligands are present.

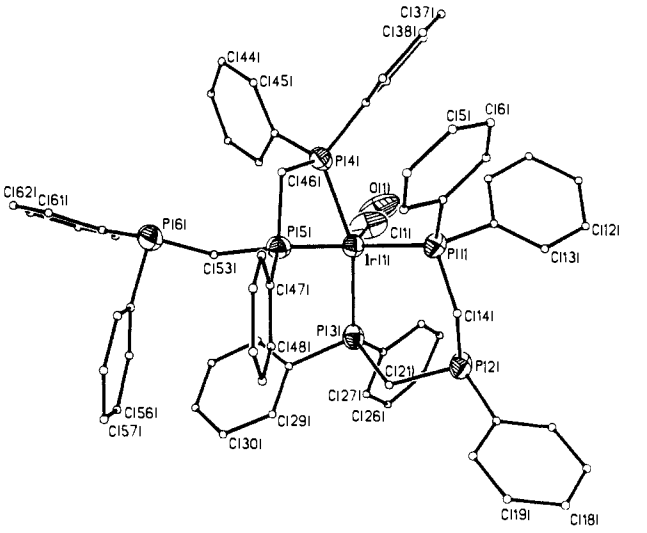

Figure 1. A perspective drawing of the cation in $[Ir(CO)(dpmp)_2][PF_6]$, **5**, using 50% thermal contours for heavy atoms and uniform, arbitrarily sized circles for carbon atoms.

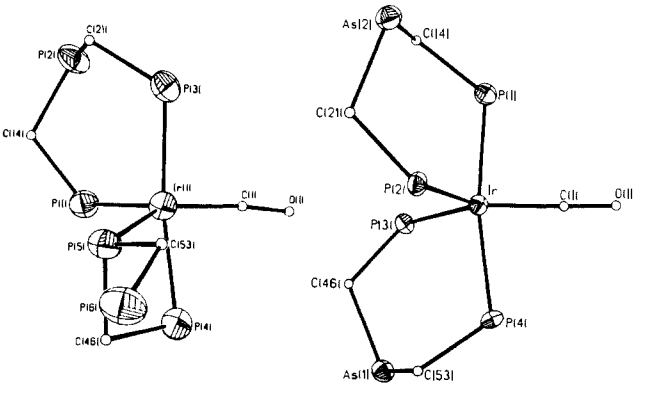

Figure 2. Comparison of the core structures for $[Ir(CO)(dpmp)_2]^+$ (left) and $[Ir(CO)(dpma)_2]^+$ (right) with the phenyl rings omitted.

Structure of $[Ir(CO)(dpmp)_2][PF_6]$ and Comparison with $[Ir(CO)(dpma)_2][PF_6]$. The asymmetric unit of $[Ir(CO)(dpmp)_2][PF_6]$ consists of the cation and the anion with no unusual contacts between them. The cation, whose structure is shown in Figure 1, has no symmetry. Selected interatomic distances and angles are given in Table I. The structure of the cation is compared with that of $[Ir(CO)(dpma)_2][PF_6]$ in Figure 2, where the inner coordination is emphasized and the ten phenyl rings on the periphery of each cation are omitted.

The two dpmp ligands in $[Ir(CO)(dpmp)_2]^+$ are bonded differently. One forms a six-membered chelate ring with its central phosphorus atom uncoordinated, while the other forms a four-membered chelate ring with a terminal phosphorus atom uncoordinated. As a result the P(4)–Ir–P(5) angle (69.3 (2)°) within the four-membered ring is severely constricted, while the P(1)–Ir–P(3) angle (97.8 (2)°) in the six-membered ring is more open. This angular distortion results in a coordination environment about iridium that is highly irregular.

In contrast, the geometry of $[Ir(CO)(dpma)_2]^+$ is much more regular. Both dpma ligands form six-membered chelate rings that leave the arsenic atoms uncoordinated. Although there is no

(5) Guimerans, R. R.; Olmstead, M. M.; Balch, A. L. *Inorg. Chem.* **1983**, *22*, 2223. Olmstead, M. M.; Guimerans, R. R.; Farr, J. P.; Balch, A. L. *Inorg. Chim. Acta* **1983**, *75*, 199. Balch, A. L.; Guimerans, R. R.; Linehan, J. *Inorg. Chem.* **1985**, *24*, 290.

Scheme I

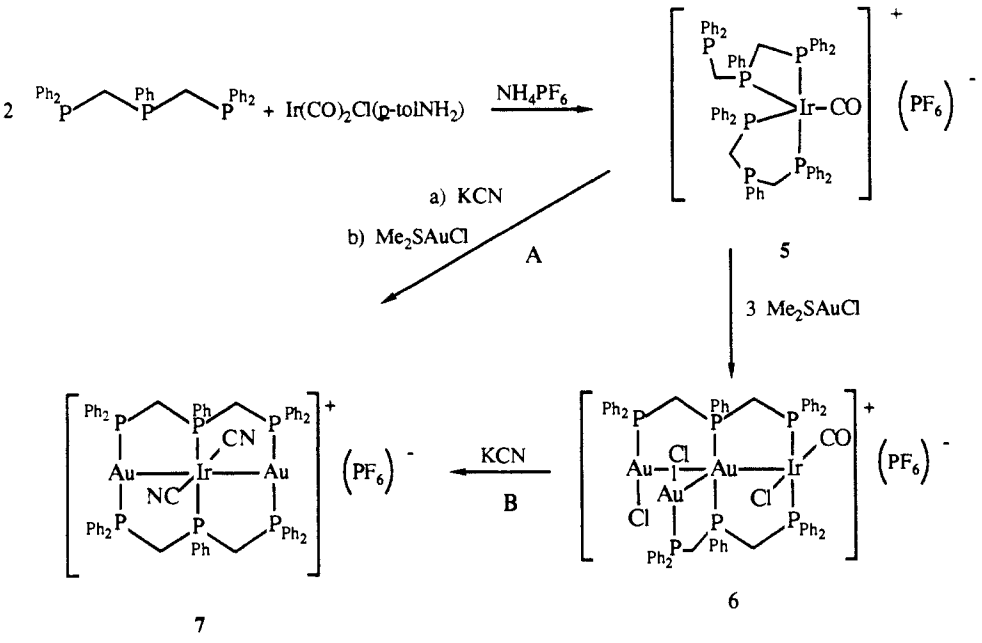

Table I. Selected Interatomic Distances and Angles for $[Ir(dpmp)_2(CO)][PF_6]$, **5**, and $[Ir(dpma)_2(CO)][PF_6]$, **3**

	$[Ir(dpmp)_2(CO)]^+$		
	Distances (Å)		
Ir–P(1)	2.362 (4)	Ir–P(3)	2.350 (4)
Ir–P(4)	2.321 (5)	Ir–P(5)	2.371 (4)
Ir–C(1)	1.82 (2)	Ir···P(2)	3.990 (4)
Ir···P(6)	5.236 (4)		
	Angle (deg)		
P(3)–Ir–P(4)	159.5 (1)	P(5)–Ir–C(1)	141.0 (7)
P(5)–Ir–P(1)	106.7 (1)	P(1)–Ir–C(1)	108.3 (6)
P(3)–Ir–P(1)	97.8 (2)	P(3)–Ir–P(5)	97.9 (1)
P(3)–Ir–C(1)	93.7 (6)	P(4)–Ir–P(1)	101.2 (1)
P(4)–Ir–C(1)	87.5 (7)	P(4)–Ir–P(5)	69.3 (2)
	$[Ir(dpma)_2(CO)]^+$		
	Distances (Å)		
Ir–P(1)	2.367 (4)	Ir–P(2)	2.400 (4)
Ir–P(3)	2.400 (4)	Ir–P(4)	2.358 (4)
Ir–C(1)	1.85 (1)	Ir···As(1)	4.316 (2)
Ir···As(2)	4.384 (2)		
	Angles (deg)		
P(1)–Ir–P(4)	169.1 (1)	P(2)–Ir–P(3)	108.1 (1)
P(2)–Ir–C(1)	127.3 (4)	P(3)–Ir–C(1)	124.6 (4)
P(1)–Ir–P(2)	91.2 (1)	P(1)–Ir–P(3)	95.9 (1)
P(1)–Ir–C(1)	85.3 (5)	P(4)–Ir–P(2)	94.0 (1)
P(4)–Ir–P(3)	91.5 (1)	P(4)–Ir–C(1)	84.0 (5)

crystallographically imposed symmetry, the $IrCP_4$ core has idealized C_{2v} symmetry (with the 2-fold axis lying along the C–Ir bond). This unit may readily be viewed as trigonal-bipyramidal with P(1) and P(4) occupying the axial sites and P(2), P(3), and C(1) occupying the equatorial positions. Thus, the P(1)–Ir–P(4) angle (169.1 (1)°) is nearly linear, and the sum of the P(2)–Ir–P(3), P(2)–Ir–C(1), and P(3)–Ir–C(1) angles is 360.0°.

Seen from the perspective of the structure of $[Ir(CO)(dpma)_2]^+$ and other complexes with $Ir(CO)P_4$ coordination,[6] the geometry of $[Ir(CO)(dpmp)_2]^+$ can also be viewed as that of a highly distorted trigonal bipyramid. In this context, P(3) and P(4) occupy the pseudoaxial sites, while P(1), P(5), and C(1) sit in the pseudoequatorial positions. Due to the constraints of the four-membered chelate ring, the P(3)–Ir–P(4) angle (159.5 (1)°) is far from linear. However, the P(1), P(5), IrC(1) group is nearly planar with the sum of the P(1)–Ir–P(5), P(1)–Ir–C(1), and P(5)–Ir–C(1) angles (356.0°) nearly 360° and the iridium ion only 0.23 Å out of the P(1), P(5), C(1) plane.

In solution, $[Ir(CO)(dpma)_2]^+$ retains its structure. Its $^{31}P\{^1H\}$ NMR spectrum at 25 °C and 121 MHz in dichloromethane consists of two triplets at −21.8 and −29.1 ppm with $J(P,P)$ = 28.8 Hz as expected for the trigonal-bipyramidal geometry. Warming it to 60 °C in acetonitrile produces minor line broadening.

The 121-MHz $^{31}P\{^1H\}$-NMR spectra of $[Ir(CO)(dpmp)_2]^+$ in chloroform at 25 °C and −60 °C are shown in Figure 3. At 25 °C six distinct phosphorus environments are readily identified. On cooling to −60 °C the spectrum becomes considerably more complex. Six major groups of resonances (those labeled A–F) can be associated with a major form which corresponds to the structure that is seen in the solid state. Resonances A and E which show strong coupling (J(A,E) = 250 Hz) are associated with the axial ligands P(3) and P(4) which are trans to one another (although a specific assignment of A to either P(3) or P(4) is not possible at this stage of the analysis). Resonance C can be assigned to the uncoordinated phosphorus P(6) since it is a simple doublet (J = 54 Hz) that is coupled only to resonance D at all temperatures. Resonance D then can be assigned to P(5) since it is coupled to P(6) and to one other phosphorus atom. Resonance B then must be due to P(1) or P(2) and resonance F to the other of those. In addition to these prominent resonances, there are other less intense peaks observed in the spectrum from −90 to −10 ppm. Some of these overlap the major resonances. For example, it is clear that there are added resonances on the low-field side of the A peaks and to the high-field side of the D resonances. Because of this overlapping and the general low intensity of these resonances, it is not possible to correlate them with a particular structure. One possibility is that this isomer is similar to **5** but with the positions of P(5), with its CH_2PPh_2 substituent, and P(4) interchanged. On warming, these resonances broaden so that by 25 °C, only the six resonance shown at the top of Figure 3 are observed. Notice that, at this stage, the large coupling seen for resonance A and E in the lower trace is lost. The fluxional process involved here probably is a pseudorotation-like motion in which the pseudotrans relationship of P(4) and P(3) is not retained but one in which P(6) remains uncoordinated. It is interesting to note that nowhere in Figure 3 is there evidence for the existence of an isomer having the structure of $[Ir(CO)(dpma)_2]^+$.

Structure and Spectroscopic Features of $[Ir(CO)ClAu(AuCl)_2(\mu\text{-dpmp})_2][PF_6]\cdot CH_2Cl_2$, 6. The structure of the cation as determined from an X-ray diffraction study is shown in Figure 4. Selected interatomic distances and angles are given in Table II. The asymmetric unit contains one cation, one entirely normal hexafluorophosphate, and one dichloromethane molecule. The

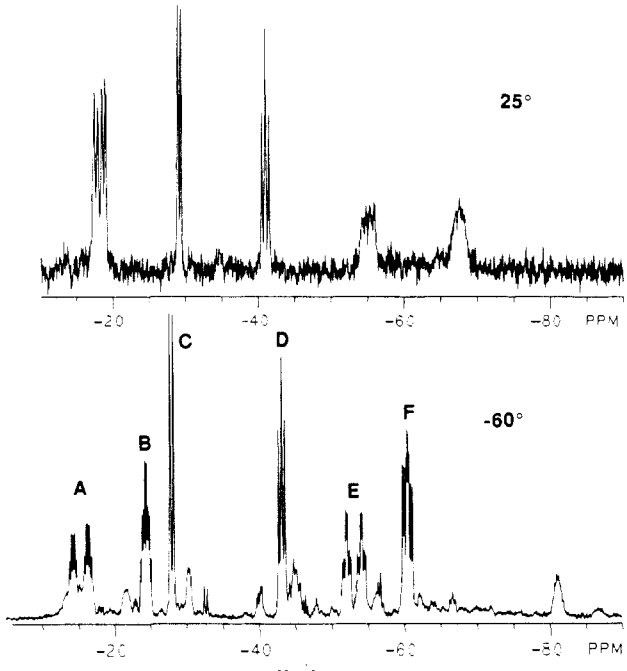

Figure 3. The 121-MHz $^{31}P\{^1H\}$-NMR spectrum of $[Ir(CO)(dpmp)_2][PF_6]$, **5**, in chloroform at 25 °C (top) and −60 °C (bottom).

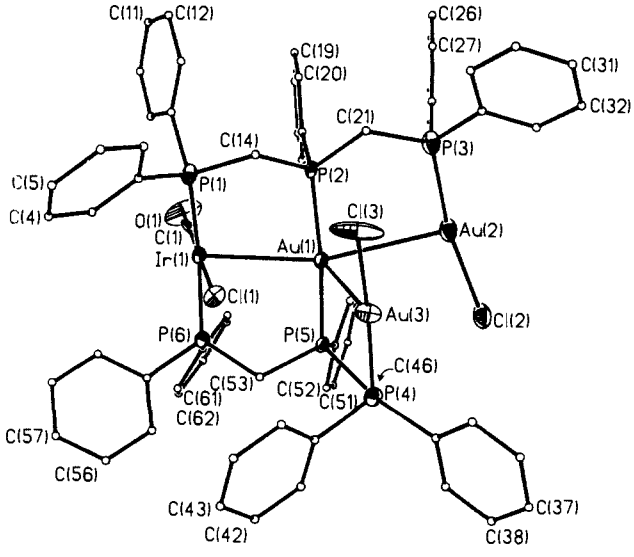

Figure 4. The structure of the cation in $[Ir(CO)ClAu(AuCl)_2(\mu\text{-dpmp})_2][PF_6]$, 6, using contours as in Figure 1. The methylene carbon, C(46), lies behind P(4).

cation contains a *trans*-Ir(CO)Cl unit attached to one end of each of the two bridging dpmp ligands to form a normal, planar Ir(CO)ClP$_2$ unit.[7] A gold ion, Au(I), is bonded to both of the central phosphorus atoms of the bridging ligands. Each of the remaining terminal phosphorus atoms are bound to AuCl units that create nearly linear P–Au–Cl portions.

The geometry of the nearly planar Ir(CO)ClAu$_3$ unit is shown in Figure 5. The Ir–Au(1)–Au(2) unit is nearly linear with Au(3) bound off to the side in a roughly T-shaped geometry. The Au(1)–Au(2) distance (3.296 (2) Å) is 0.2 Å longer than the Au(1)–Au(3) distance (3.097 (2) Å), but both are less than 3.5 Å, the distance at which Jones has characterized as remarkably short for such large ions.[8] The coordination environment of Au(1)

Table II. Selected Interatomic Distances and Angles in $[Ir(CO)ClAu(AuCl)_2(\mu\text{-dpmp})_2][PF_6]$, 6

		Distances (Å)	
		At–Ir	
Ir(1)–Au(1)	3.115 (2)		
Ir(1)–P(1)	2.326 (7)	Ir(1)–P(6)	2.318 (7)
Ir(1)–C(1)	1.789 (21)	Ir(1)–Cl(1)	2.364 (6)
		At–Au(I)	
Au(1)–Ir(1)	3.115 (2)	Au(1)–Au(2)	3.296 (2)
Au(1)–Au(2)	3.296 (2)	Au(1)–Au(3)	3.097 (2)
Au(1)–P(2)	2.324 (7)	Au(1)–P(5)	2.325 (7)
		At–Au(2)	
Au(2)–Au(1)	3.296 (2)	Au(2)···Au(3)	3.703 (2)
Au(2)–P(3)	2.241 (8)	Au(2)–Cl(2)	2.313 (8)
		At–Au(3)	
Au(3)–Au(1)	3.097 (2)	Au(3)··Au(2)	3.703 (2)
Au(3)–P(4)	2.241 (7)	Au(3)–Cl(3)	2.295 (11)
		Angles (deg)	
		At–Ir	
Au(1)–Ir(1)–P(1)	93.1 (2)	Au(1)–Ir(1)–Cl(1)	72.3 (2)
Au(1)–Ir(1)–P(6)	89.4 (2)	Au(1)–Ir(1)–C(1)	107.8 (4)
P(1)–Ir(1)–P(6)	169.6 (2)	Cl(1)–Ir(1)–C(1)	180.0 (12)
P(1)–Ir(1)–Cl(1)	84.5 (2)	P(6)–Ir(1)–Cl(1)	86.6 (2)
P(1)–Ir(1)–C(1)	95.6 (9)	P(6)–Ir(1)–C(1)	93.3 (9)
		At–Au(1)	
Ir(1)–Au(1)–Au(2)	164.9 (1)	Ir(1)–Au(1)–Au(3)	116.3 (1)
Au(2)–Au(1)–Au(3)	70.7 (1)	P(2)–Au(1)–P(5)	170.5 (2)
		At–Au(2)	
Au(1)–Au(2)–P(3)	92.1 (2)	Au(1)–Au(2)–Cl(2)	98.2 (2)
Cl(2)–Au(2)–P(3)	169.0 (3)		
		At–Au(3)	
Au(1)–Au(3)–P(4)	92.9 (2)	Au(1)–Au(3)–Cl(3)	94.1 (2)
Cl(3)–Au(3)–P(4)	170.1 (3)		

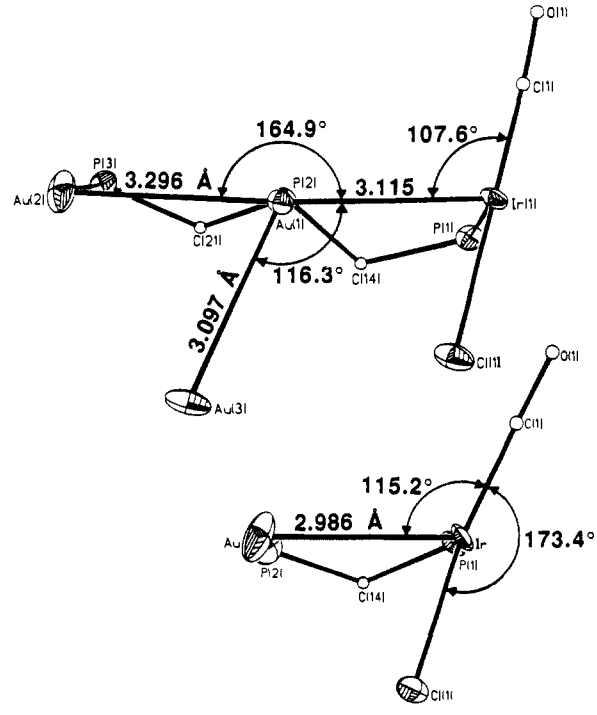

Figure 5. Comparison of similar sections of (top) $[Ir(CO)ClAu(AuCl)_2(\mu\text{-dpmp})_2]^+$ and (bottom) $[Ir(CO)ClAu(\mu\text{-dpm})_2]^+$. The phenyl rings and the upper bridging phosphine ligand have been omitted.

is all the more unusual since it is in close contact with not only the other two gold ions but with the iridium ion as well. To our

(6) Miller, J. S.; Caulton, K. G. *J. Am. Chem. Soc.* **1975**, *97*, 1067. Sanger, A. R. *J. Chem. Soc.* **1977**, 1979.
(7) Churchill, M. R.; Feltinger, J. C.; Buttrey, L. A.; Barkam, M. D.; Thompson, J. S. *J. Organomet. Chem.* **1988**, *340*, 257.
(8) Jones, P. G. *Gold Bull.* **1981**, *14*, 102; **1981**, *14*, 159; **1983**, *16*, 114; **1986**, *19*, 46.

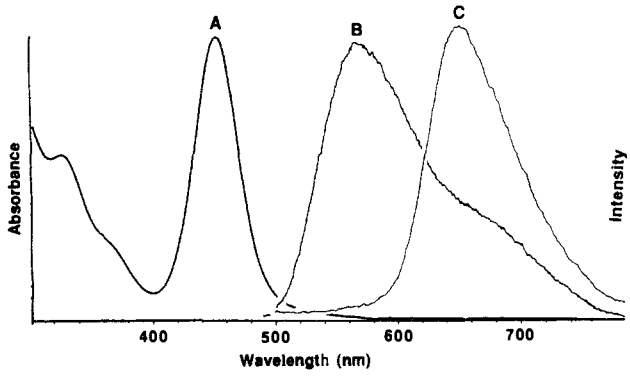

Figure 6. The electronic absorption at 23 °C (A) and uncorrected emission spectra at 23 °C (B) and at 77 K (C) of $[Ir(CO)ClAu(AuCl_2)(\mu\text{-dpmp})_2][PF_6]$ in dichloromethane.

knowledge, this is the first example of an Au(I) ion that is in close proximity with three other metal ions.

The right-hand portion of $[Ir(CO)ClAu(AuCl)_2(\mu\text{-dpmp})_2]^+$ is closely related to the simple binuclear complex, $[Ir(CO)ClAu(\mu\text{-dpm})_2][PF_6]$, **8** (where dpm is bis(diphenylphosphino)-

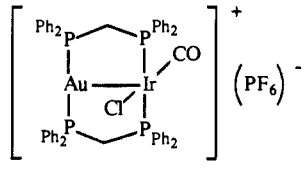

8

methane).[9] The two structures can be compared by turning to Figure 5. The Ir–Au distance in **6** is somewhat longer than that in **8**. In both, the position of the gold ion lies off to the side of the chloride ligand on iridium; thus the Au–Ir–Cl angles are less than 90° in both cases. The methylene bridges in both complexes lie to the same side, the side of the chloride ligand on the iridium. Thus, the P_4C_2 portion in both complexes assumes a boat rather than a chair conformation.

The electronic spectral properties of these two complexes are also similar which suggests that the basic chromophore is the AuIr unit. The absorption spectrum of **6** in dichloromethane solution is shown in trace A of Figure 6. The intense absorption at 454 nm (ϵ = 9500 M^{-1} cm^{-1}) is assigned to a $\sigma^*(d_{z^2},d_{z^2},d_{z^2}) \rightarrow \sigma(p_z,p_z,p_z)$ transition that is delocalized along the nearly linear AuAuIr unit. The shift of this transition to lower energy (from 440 nm in **8**)[9] is a consequence of the involvement of three metal ions within the chromophore. Trace B of Figure 6 shows the emission spectrum of **6** obtained in dichloromethane at 23 °C, while trace C shows the emission spectrum obtained at 77 K in a frozen dichloromethane solution. The two emission bands seen at 568 and 660 nm in trace B are assigned to fluorescence and phosphorescence, respectively. The increase in the relative intensity of the low-energy band relative to the high-energy emission that occurs when the sample is cooled to 77 K is similar to what is observed for related compounds including both **4** and **8**. This increase is attributed to reduction of temperature-dependent quenching of the phosphorescence at low temperature.[11] Attempts to measure the lifetimes of the excited states responsible for these emissions have been thwarted by the ease with which **6** decomposes (with deposition of metallic gold) in a laser beam.

Structure and Spectroscopic Properties of $[Ir(CN)_2Au_2(\mu\text{-dpmp})_2][PF_6]\cdot 2C_7H_8\cdot 0.5CH_2Cl_2$, 7. The asymmetric unit of the crystal consists of one-half of the cation, a hexafluorophosphate ion at half occupancy, one toluene molecule, and a dichloro-

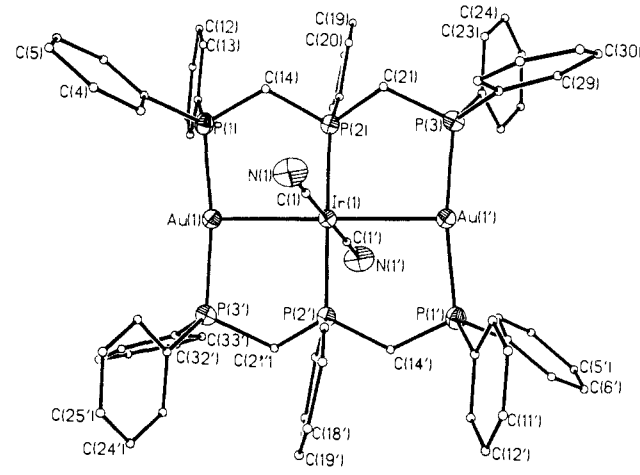

Figure 7. The structure of the cation in $[Ir(CN)_2Au_2(\mu\text{-dpmp})_2][PF_6]\cdot 2C_7H_8$, **7**, with thermal contours as described in Figure 1.

Table III. Selected Interatomic Distances and Angles for $[Au_2Ir(CN)_2(\mu\text{-dppp})_2][PF_6]$, **7**

	Distances (Å)		
	At–Au(1)		
Au(1)–Ir(1)	2.835 (1)		
Au(1)–P(1)	2.303 (5)	Au(1)–P(3A)	2.309 (5)
	At–Ir(1)		
Ir(1)–Au(1)	2.835 (1)	Ir(1)–P(2)	2.300 (5)
Ir(1)–C(1)	2.005 (17)	N(1)–C(1)	1.15 (21)
	Angles (deg)		
	At–Au(1)		
Ir(1)–Au(1)–P(1)	94.7 (1)	Ir(1)–Au(1)–P(3A)	94.2 (1)
P(1)–Au(1)–P(3A)	171.1 (1)		
	At–Ir(1)		
Au(1)–Ir(1)–Au(1A)	180	Au(1)–Ir(1)–P(2A)	90.3 (1)
Au(1)–Ir(1)–C(1)	85.3 (4)	Au(1)–Ir(1)–P(2)	89.7 (1)
Au(1)–Ir(1)–C(1A)	94.7 (4)	P(2)–Ir(1)–P(2A)	180
P(2)–Ir(1)–C(1)	82.9 (5)	P(2)–Ir(1)–C(1A)	97.1 (5)
C(1)–Ir(1)–P(2A)	97.1 (5)	C(1)–Ir(1)–C(1A)	180

methane molecule at one-quarter occupancy. There are no abnormal interactions between these moieties. The structure of one entire cation is reproduced in Figure 7, and selected interatomic distances and angles are set out in Table III.

The cation, which consists of a planar $Ir(CN)_2P_2$ unit flanked by two nearly linear P–Au–P units, has a crystallographically imposed center of symmetry. Consequently, the two Au–Ir distances are identical. This distance (2.835 (1) Å) is shorter than the corresponding distances in $[Ir(CO)ClAu_2(\mu\text{-dpma})_2][PF_6]$, **4** (3.014 (2), 3.013 (2) Å),[4] in $[Ir(CO)ClAu(AuCl)_2(\mu\text{-dpmp})_2][PF_6]$, **6**, in $[Ir(CO)ClAu(\mu\text{-dpm})_2][PF_6]$, **8** (2.986 (1) Å),[9] or $[Ir_2(CO)_2Cl_2Au(\mu\text{-dpma})_2][BPh_4]$, **9** (3.059 (1) Å).[12]

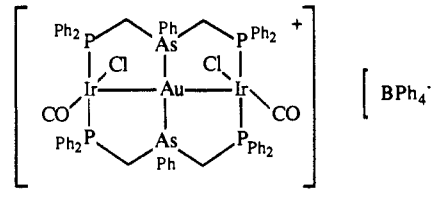

9

Nevertheless, it is longer than the expected range (2.59–2.8 Å)

(9) Balch, A. L.; Catalano, V. J.; Olmstead, M. M. *Inorg. Chem.* **1990**, *29*, 585.
(10) Balch, A. L.; *J. Am. Chem. Soc.* **1976**, *98*, 8049.
(11) Kenney, M. I. S.; Kenney, J. W., III; Crosby, G. A. *Organometallics* **1986**, *5*, 230.
(12) Balch, A. L.; Nagle, J. K.; Oram, D. E.; Reedy, Jr., P. E. *J. Am. Chem. Soc.* **1988**, *110*, 454.

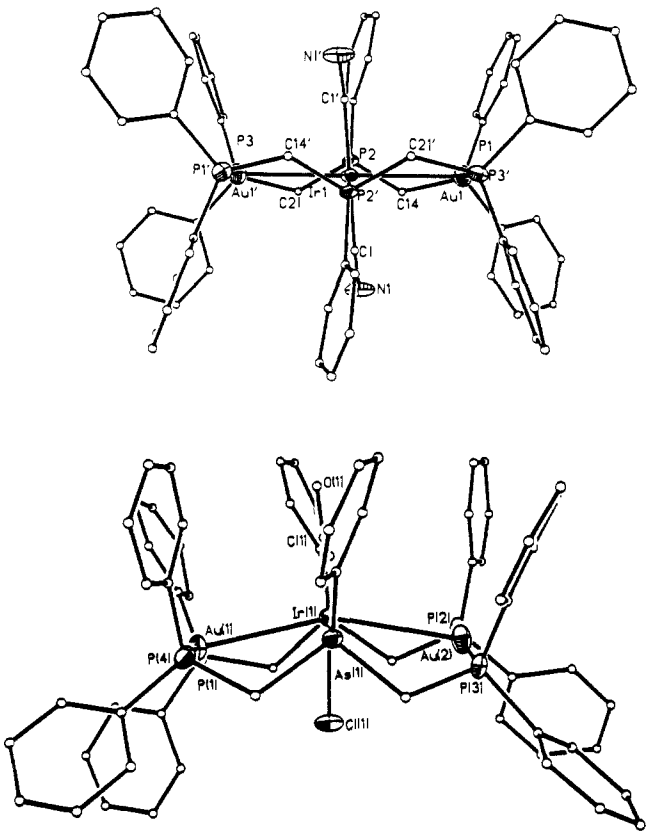

Figure 8. Comparison of structures of (top) $[Ir(CN)_2Au_2(\mu\text{-dpmp})_2]^+$ and (bottom) $[Ir(CO)ClAu_2(\mu\text{-dpma})_2]^{2+}$.

for normal, two-electron Au–Ir single bonds.[13] As a consequence of the center of symmetry, the trans angles at iridium (C–Ir–C, P–Ir–P, and Au–Ir–Au) are all 180°. However, the NC–Ir–CN unit is canted with respect to the Au–Ir–Au framework so that the Au–Ir–C angle is 85.2 (4)°. The P–Au–P units are slightly bent (171.1 (1)°) with the direction of the bend facilitating the close approach of the gold ions to the central iridium.

The dpmp ligands in doubly-bridged trinuclear complexes can be arranged in two distinct fashions.[14] These are shown in Newman projections down the P–Ir–P axes as **10** (cis) and **11** (trans). These two arrangements are very similar to the well-

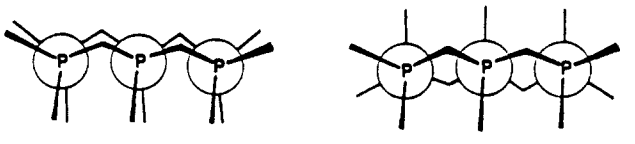

10 (cis) **11** (trans)

known *cis*- and *trans*-decalin structures with the P–Ir–P units replacing C–C portions. Figure 8 shows the core structure of $[Ir(CN)_2Au_2(\mu\text{-dpmp})_2]^+$ seen from a vantage point that emphasizes the relative orientation of the two dpmp ligands. A corresponding view of $[Ir(CO)ClAu_2(\mu\text{-dpma})_2]^{2+}$[4] is also shown. $[Ir(CN)_2Au_2(\mu\text{-dpmp})_2]^+$ is unusual since it has the two dpmp ligands in the trans arrangement, whereas all other trinuclear complexes with two dpmp or dpma bridges that have been characterized in this laboratory to date have the cis arrangement.

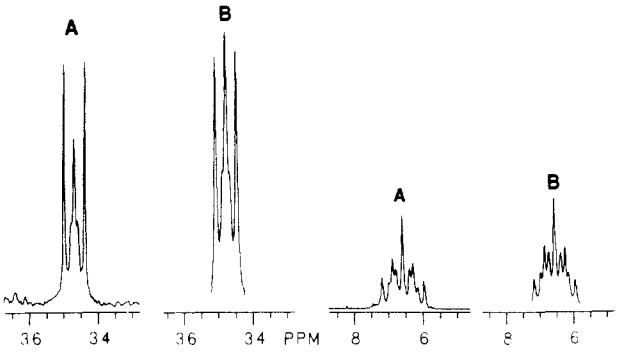

Figure 9. The 121-MHz $^{31}P\{^1H\}$-NMR spectrum of (A) $[Ir(CN)_2Au_2(\mu\text{-dpmp})_2][PF_6]$ in chloroform solution at 23 °C and (B) simulated spectrum using parameters described in the text.

The trans arrangement produces a degree of structural rigidity to this cation that is not present in $[Ir(CO)ClAu_2(\mu\text{-dpma})_2]^+$ or in any of the other known doubly-bridged trinuclear species. In effect, the two bridges in $[Ir(CN)_2Au_2(\mu\text{-dpmp})_2]^+$ are juxtaposed like two opposing springs that limit bending of the Au–Ir–Au chain. In contrast, in complexes containing the cis orientation, such a counterbalancing of forces is not present and bending of the M_3 chain is more readily accomplished.

The $^{31}P\{^1H\}$-NMR spectrum of **7** shown in Figure 9 is relatively simple. It consists of a symmetrical multiplet at 34.7 ppm (5 lines, intensity 4) and a second symmetrical multiplet at 6.5 ppm (11 lines, intensity 2). A satisfactory simulation of the spectrum can be achieved by assuming two values for $J(P^t,P^i)$ of 26 and 12 Hz (where P^t and P^i represent the terminal and internal phosphorus atoms) and trans-$J(P^t,P^t)$ and $J(P^i,P^i)$ values in the range 150–350 Hz. These spectroscopic features are entirely in accord with the structure of **7** that has been determined by X-ray crystallography.

Trace A of Figure 10 shows the electronic absorption spectrum of $Ir(CN)_2Au_2(\mu\text{-dpmp})_2][PF_6]$ in dichloromethane solution. An intense band at 578 nm (ϵ = 15 800 M^{-1} cm^{-1}) is responsible for the magenta color of this complex. In comparison $[Ir(CO)ClAu_2(\mu\text{-dpma})_2][PF_6]$ has a similar spectrum, but the intense absorption occurs at higher energy, 498 nm. These electronic spectral features can be interpreted in terms of a modification (to a $d^{10}d^8d^{10}$, $Au^IIr^IAu^I$ chain) of the qualitative molecular orbital picture developed for the nearly linear $d^8d^{10}d^8$ Ir^I–Au^I–Ir^I chain in $[Ir_2(CO)_2Cl_2Au(\mu\text{-dpma})_2][BPh_4]$, **9**.[12] In such chains the predominant interactions involve the filled d_{z^2} and empty p_z orbitals that are directed along the Au–Ir–Au axis.[4] The shift of the intense absorption to lower energy in **7** (relative to **9**) is consistent with the shorter Au–Ir distances in **7**.[10,15] The shift may also be partly due to the change in terminal ligands (from two CN^- to CO and Cl^-). It is not expected that the change from phosphorus to arsenic donors in the iridium has a major spectral effect.[16] Trace B of Figure 10 shows the emission spectrum of a dioxygen-free solution of **7** at 25 °C, while trace C shows the emission spectrum obtained at 77 K. The intense emission at 612 nm is assigned at fluorescence on the basis of its small Stokes' shift, while the lower energy emission at 782 nm is assigned as phosphorescence. The lifetimes of these emissions are consistent with these assignments. At 25 °C in dichloromethane solution the low-energy emission has a lifetime of 6.7 μs, while the higher energy emission has a lifetime of 0.2 ns. In contrast to the situation with **6**, cooling results in a decrease in the relative intensity of the low-energy emission. This behavior may result from an absolute enhancement of the fluorescence intensity at low temperatures. Because of the structural rigidity of **7** that is brought about by the disposition of the two dpmp bridges, it is not surprising that there may be little or no temperature-dependent quenching of the phosphorescence for this ion. This rigidity of **7** also accounts for the fact that the lifetime of the low-energy emission seen for **7** is an order of magnitude larger than that observed for **4**.[4]

(13) Casalnuova, A. L.; Pignolet, L. H.; van der Velden, J. W. A.; Bour, J. J.; Steggerda, J. J. *J. Am. Chem. Soc.* **1983**, *105*, 5957. Casalnuova, A. L.; Laska, R.; Nilsson, P. V.; Olofson, J.; Pignolet, L. H. *Inorg. Chem.* **1985**, *24*, 233. Casalnuova, A. L.; Casalnuova, J. A.; Nilsson, P. V.; Pignolet, L. H. *Inorg. Chem.* **1985**, *24*, 2554. Casalnuova, A. L.; Laska, T.; Nilsson, P. V.; Olofson, J.; Pignolet, L. H.; Bos, W.; Bour, J. J.; Steggerda, J. J. *Inorg. Chem.* **1985**, *24*, 182.

(14) Balch, A. L.; Fossett, L. A.; Guimerans, R. R.; Olmstead, M. M. *Organometallics* **1985**, *4*, 781.

(15) Balch, A. L.; Tulyathan, B. *Inorg. Chem.* **1977**, *16*, 2840.

(16) Fordyce, W. A.; Crosby, G. A. *J. Am. Chem. Soc.* **1982**, *104*, 985.

Table IV. Crystallographic Data

	4	6	7
	$[Ir(CO)(dpmp)_2][PF_6]$	$[Ir(CO)ClAu(AuCl)_2(dpmp)_2][PF_6]$	$[Au_2Ir(CN)_2(dpmp)_2][PF_6]$
formula	$C_{65}H_{53}IrF_6P_7$	$C_{66}H_{60}Au_3Cl_5F_6IrOP_7$	$C_{80.5}H_{75}Au_2ClF_6IrN_2P_7$
formula weight	1372.6	2160.4	2022.9
color and habit	yellow plates	red triangular prism	purple blocks
crystal system	triclinic	orthorhombic	triclinic
space group	$P\bar{1}$	$P2_1/n$	$P\bar{1}$
a, Å	11.948 (7)	16.584 (5)	12.291 (2)
b, Å	12.133 (5)	18.960 (10)	12.479 (3)
c, Å	22.558 (11)	23.314 (10)	15.513 (4)
α, deg	84.16 (4)	90.00	109.19 (2)
β, deg	85.02 (4)	96.97 (3)	109.38 (2)
γ, deg	65.55 (4)	90.00	99.19 (2)
V, Å^3	2957 (3)	7245 (5)	2021 (1)
T, K	130	130	130
Z	2	4	1
cryst dimens, mm	0.05 × 0.25 × 0.38	0.17 × 0.23 × 0.22	0.15 × 0.20 × 0.50
d_{calcd}, g cm^{-3}	1.54	1.98	1.66
radiation, Å	Mo Kα (λ = 0.71069)	Mo Kα (λ = 0.71069)	Mo Kα (λ = 0.71069)
μ(Mo Kα), cm^{-1}	26.37	83.42	55.80
range of transm factors	0.42–0.91	0.199–0.294	0.109–0.495
diffractometer	Syntex $P2_1$	Syntex $P2_1$	Syntex $P2_1$
scan method	ω scan	ω scan	ω scan
scan range, deg	1.0	1.2	1.1
background offset, deg	1.0	1.0	1.1
scan speed, deg min^{-1}	8.0	12.0	8.0
2θ range, deg	0–50	0–50	0–50
octants collected	4	1	4
no. data collected	10458	13363	7081
no. unique data	6255	7235	5222
	R(merge) = 0.0406	R(merge) = 0.0111	[R(merge) = 0.0115]
no. data refined	5272 [$I > 4\sigma(I)$]	7232 [$I > 6\sigma(I)$]	4722 [$I > 4\sigma(I)$]
no. parameters refined	389	314	278
R^a	0.0734	0.0834	0.0655
$R_w{}^a$	0.0719 [$w = 1/(\sigma^2 F_o)$]	0.0878 [$w = 1/(\sigma^2 F_o)$]	0.0713 [$w = 1/\sigma^2(F_o)$]

$^a R = \sum||F_o| - |F_c||/|F_o|$ and $R_w = \sum||F_o| - |F_c||w^{1/2}/\sum|F_o w^{1/2}|$.

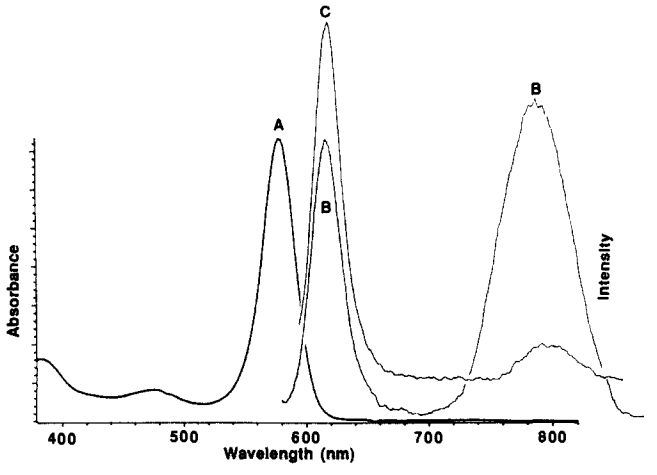

Figure 10. The electronic absorption (A) and uncorrected emission (B) spectra of $[Ir(CN)_2Au_2(\mu\text{-dpmp})_2][PF_6]\cdot 2C_7H_8$ in dichloromethane at 23 °C. The emission spectrum recorded for a sample at 77 K is shown in (C).

Discussion

The reactions described here and summarized in Scheme I demonstrate that a remarkable amount of metal–ligand bond breaking and making is involved in these transformations. In this regard, they contrast strongly with the now predictable behavior of the metallomacrocycles such as **1** where complexation into the central cavity has so far always resulted in retention of the cyclic structure.[1]

The variation in structures between $[Ir(CO)(dpmp)_2][PF_6]$, **5**, and $[Ir(CO)(dpma)_2][PF_6]$, **3**, reveals how delicately these structural types are poised relative to one another. This is not entirely unexpected and may be related to steric factors occurring within the metal ion coordination sphere. Thus, there is a variation of coordination mode of dpma and dpmp with coordination number. For the four-coordinate $Au(dpma)_2^+$ with low steric congestion, both ligands adopt the six-membered P,P-chelate form.[17] In the more crowded, six-coordinate $Ru(dpma)_2Cl_2$, the two ligands exist in two different forms. One forms a six-membered chelate, while the other forms a four-membered ring with coordination through one phosphorus and one arsenic.[17] With five-coordinate iridium, with its intermediate steric congestion, the factors are balanced so that either situation can occur.

The observation of the different structures for $[Ir(CO)(dpma)_2][PF_6]$, **3** and $[Ir(CO)(dpmp)_2][PF_6]^+$, **5** offers a possible explanation for the ring opening reactions seen in eq 2 and Scheme I. The body of work due to Shaw and co-workers has already demonstrated that strained, four-membered chelate rings such as those found in $[Ir(CO)(dpm)_2][PF_6]$ are readily opened through the addition of other metal ions.[18] Thus, in $[Ir(CO)(dpmp)_2][PF_6]$ the dpmp ligand that forms a four-membered chelate ring offers two sites for attack by Me_2SAuCl: the dangling phosphorus atom and the chelate ring itself. Note that attack on the chelate ring then can occur so that iridium ends up attached to the terminal phosphorus atom (as seen in Scheme I for formation of **5**) or to the middle phosphorus atom. These considerations lead to the suggestion that there may exist an equilibrium between the six- and four-membered chelating forms of both dpmp and dpma. The four-membered forms are likely to be the ones that are most reactive toward other metal ions and critical for the formation of polynuclear complexes. Thus, reaction 2 may be facilitated by the presence of a small amount (too small for spectroscopic detection) of an isomer of $[Ir(CO)(dpma)_2][PF_6]$ that has a structure that is analogous to that of $[Ir(CO)(dpmp)_2][PF_6]$, that is, a structure with one four-membered chelate ring.

(17) Balch, A. L.; Olmstead, M. M.; Reedy, Jr., P. E.; Rowley, S. P. *Inorg. Chem.* **1988**, *27*, 4289.

(18) McEwan, D. M.; Pringle, P. G.; Shaw, B. L. *J. Chem. Soc., Chem. Commun.* **1982**, 1240. Blagg, A.; Cooper, G. R.; Pringle, P. G.; Robson, R.; Shaw, B. L. *J. Chem. Soc., Chem. Commun.* **1984**, 933. Hutton, A. T.; Pringle, P. G.; Shaw, B. L. *Organometallics* **1983**, *2*, 1889.

The transformation of **5** into **6** produces a new structural type of complex in which the two dpmp ligands span four metal ions in a bifurcated fashion. Despite the proximity of four metal centers in this novel species, there is a great similarity in structural and spectroscopic features in **6** and the binuclear complex **8**. While structure **6** is unusual, it appears to have good stability. In related work we have prepared and structurally characterized two other complexes that have this bifurcated structure, $[Ir(CO)ClAu(AuCl)_2(\mu\text{-dpma})_2][PF_6]$ and $[Ir(CO)ClAu(AuPh)_2(\mu\text{-dpma})_2][BPh_4]$. A related tetranuclear complex, $PdCl_2(PhAs(CH_2PPh_2AuCl)_2]_2$, which contains a trans As–Pd–As unit, also has been thoroughly characterized and represents an extreme in opening up of the bis(dpma) or bis(dpmp) framework to accommodate additional binding of Au–Cl groups.[19]

The transformation of **6** into **7** represents the first case of apparent migration of two metals between sites in a ligand-bridged complex of this type. The reorganization involved in going from **6** to **7** requires, of course, much more than interchange of a gold and an iridium within the complex since the relative orientation of the phosphine ligands changes, and a gold ion is lost from the complex. The finding of two routes to the formation of **7** and the number of bond-breaking and -making steps in each suggests that this is the thermodynamically favored product. The structural and spectroscopic similarities in related complexes including **2**, **4**, **6**, **7**, and **8** demonstrate that the planar d^8 and linear d^{10} units may be considered as interchangeable units that can be readily incorporated into such polynuclear complexes. The facility of forming the array of complexes shown in eq 2 and Scheme I with the heavy elements iridium and gold may result from relativistic effects that strengthen metal–metal bonding in this section of the periodic table.[20-22] In this regard, we have recently reported an example where weak attractive interaction between gold(I) centers play a role in guiding a chemical reaction.[23] The transformations in Scheme I may similarly be guided by weak Ir···Au associations.

Experimental Section

Preparation of Compounds. $Ir(CO)_2Cl(p\text{-toluidine})$,[24] Me_2SAuCl,[25] dpma,[2] and dpmp[26] were prepared by standard routes. The new compounds described here are stable to moisture and dioxygen and can be prepared without recourse to inert atmosphere techniques.

$[Ir(CO)(dpma)_2][PF_6]$, 3. Fifty milligrams (0.128 mmol) of $Ir(CO)_2Cl(p\text{-}C_7H_7NH_2)$ dissolved in 20 mL of methanol and 10 mL of dichloromethane was mixed with 142 mg (0.258 mmol) of dpma to produce a pale yellow solution. After stirring the solution for 20 min, 50 mg (0.307 mmol) of ammonium hexafluorophosphate dissolved in a minimum volume of methanol was added. The volume was reduced until crystals of a pale ivory compound formed. The product was collected by filtration and recrystallized from CH_2Cl_2/diethyl ether (yield: 76%).

$[Ir(CO)(dpmp)_2][PF_6]$, 5. A solution of 300 mg (0.592 mmol) of dpmp in 25 mL of dichloromethane and 75 mL of methanol was added to 100 mg (0.256 mmol) of $Ir(CO)_2Cl(p\text{-}C_7H_7NH_2)$ and 200 mg (1.23 mmol) of ammonium hexafluorophosphate. The solution became red and then turned yellow upon stirring. After stirring for 20 min, the volume was reduced under vacuum to yield a yellow crystalline solid. The solid was collected by filtration. It was purified by dissolving it in a minimum volume of dichloromethane, filtering the solution, and precipitating the product by the gradual addition of ethyl ether (yield: 61%).

$[Ir(CO)ClAu(AuCl)_2(\mu\text{-dpmp})_2][PF_6]$, 6. To 50 mg (0.036 mmol) of $[Ir(CO)(dpmp)_2][PF_6]$ dissolved in 20 mL of dichloromethane was added 32 mg (0.109 mmol) of $(Me_2S)AuCl$ to produce a bright red-orange solution. The solution is allowed to stir for 10 min after which the volume was reduced under vacuum to 10 mL. Addition of diethyl ether afforded an orange solid which was collected and washed with diethyl ether. The solid was recrystallized by dissolving it in a minimum volume of dichloromethane, filtering the solution, and adding ethyl ether to precipitate the product from the filtrate (yield: 85%).

$[Au_2Ir(CN)_2(\mu\text{-dpmp})_2][PF_6]$, 7. (A) From $[Ir(CO)ClAu(AuCl)_2(\mu\text{-dpmp})_2][PF_6]$. A 0.96-mL (0.096 mmol) portion of a 0.1 M potassium cyanide solution in methanol was added to 50 mg (0.024 mmol) of $[Ir(CO)ClAu(AuCl)_2(\mu\text{-dpmp})_2][PF_6]$ dissolved in 10 mL of dichloromethane. The initial orange solution turned red and became deep magenta after stirring. The solution was filtered through Celite, and 10 mg (0.061 mmol) of ammonium hexafluorophosphate in 5 mL of methanol was added. Reduction of the solvent volume and addition of diethyl ether afforded deep purple crystals (yield: 70%).

(B) From $[Ir(CO)(dpmp)_2][PF_6]$. A 1.08-mL (0.108 mmol) portion of a 0.1 M potassium cyanide solution in methanol was added to a pale yellow solution of 50 mg (0.036 mmol) of $[Ir(CO)(dpmp)_2][PF_6]$, **5**, in 10 mL of dichloromethane. The solution became bright yellow. Addition of 21 mg (0.072 mmol) of $(Me_2S)AuCl$ caused the solution to turn deep magenta. The solution was stirred for 10 min and then filtered through Celite. Reduction of the solvent volume and addition of 10 mg (0.061 mmol) of ammonium hexafluorophosphate in 5 mL of methanol afforded deep purple crystals (yield: 71%).

Physical Measurements. The $^{31}P\{^1H\}$ NMR spectra were recorded on a General Electric QE-300 NMR spectrometer that operates at 121.7 MHz with an external 85% phosphoric acid standard and the high field positive convention for reporting chemical shifts. Infrared spectra were recorded on an IBM IR32 spectrometer. Electronic spectra were recorded with a Hewlett-Packard 8450A spectrometer. Uncorrected emission spectra were obtained through the use of a Perkin-Elmer MPF-44B fluorescence spectrometer.

Standard laser induced fluorescence (LIF) techniques were employed to measure excited-state lifetimes with 355- and 532-nm excitation from a Nd:YAG laser operating at 20 Hz with a pulse duration of 10 ns at 1 mJ per pulse. Emitted light was collected using a 4-in. parabolic mirror and focused into an Acton VM-510 1-meter monochromator. Emissions were monitored at their λ_{max} of emission. Luminescence was detected by a Hamamatsu R1477 PMT. Output was directed to a E.G.&G Model 162 Boxcar averager. Scans were collected over a 20-μs range and averaged for 100 s with an average gatewidth of 5 ns. Intensity traces were collected on a X-Y recorder where they were analyzed for first-order decay over at least 10 half-lives. The fluorescence lifetime for $[Au_2Ir(CN)_2(\mu\text{-dpmp})_2][PF_6]$ was measured by an ISS K2 multifrequency phase fluorometer. In each case the solvent was dichloromethane that was freshly distilled from calcium hydride. Sample concentrations were on the order of 10^{-4} molar. Solvent was degassed by using four freeze–pump–thaw cycles.

X-ray Crystallographic Studies. $[Ir(CO)(dpmp)_2][PF_6]$. The yellow plates were formed by slow diffusion of diethyl ether into a dichloromethane solution of $[Ir(CO)(dpmp)_2PF_6]$. The air-sensitive crystals were coated with a light hydrocarbon oil to prevent cracking. The crystal was mounted on a glass fiber with silicon grease and placed into the 130 K nitrogen stream of a Syntex $P2_1$ diffractometer equipped with a modified LT-1 low-temperature apparatus. Unit cell parameters were determined by least-squares refinement of 11 reflections with $10 < 2\theta < 21°$. The two check reflections exhibited only random (<2%) fluctuations throughout the data collection. The data were corrected for Lorentz and polarization effects. Crystal data are given in Table IV.

Calculations were performed with SHELXTL, version 5, installed on a Data General MV/10000 computer. Scattering factors and corrections for anomalous dispersion were taken from a standard source.[27] The structure was solved by Patterson techniques. An absorption correction was applied.[28] Final refinement was carried out with anisotropic thermal parameters for iridium, arsenic, chlorine, oxygen, and phosphorus atoms and isotropic parameters for carbon (except for C(1)). The phenyl ring, C(15)–C(20), was refined as a rigid group, while all other rings were unconstrained. Hydrogens were fixed to all carbons except C(1) and C(15)–C(20). The hydrogen atom positions were calculated by using a riding model with a C–H vector fixed at 0.96 Å and a thermal parameter 1.2 times the host carbon. The largest peak in the final difference map had density equal to 1.8 electrons/Å^3. This peak is 0.761 Å from C(17). The goodness of fit was calculated at 1.577.

$[Ir(CO)ClAu(AuCl)_2(\mu\text{-dpmp})_2][PF_6]\cdot 2C_7H_8\cdot 0.5CH_2Cl_2$. Orange crystals were obtained by slow diffusion of diethyl ether into a dichloromethane solution of $[Ir(CO)ClAu(AuCl)_2(\mu\text{-dpmp})_2][PF_6]$ and handled as described above. Unit cell parameters were determined by least-squares refinement of 11 reflections with $13 \le 2\theta < 23°$. The space group was determined to be $P2_1/n$ (No. 14) from the observed conditions $(h0l)$, $h + l = 2n$ and $(0k0)$, $k = 2n$. The two check reflections showed

(19) Balch, A. L.; Fung, E. Y.; Olmstead, M. M., *Inorg. Chem.* In press.
(20) Pyykkö, P.; Declaux, J.-P. *Acc. Chem. Res.* **1979**, *12*, 276.
(21) Pitzer, K. S. *Acc. Chem. Res.* **1979**, *12*, 271.
(22) Pyykkö, P. *Chem. Rev.* **1988**, *88*, 563.
(23) Balch, A. L.; Fung, E. Y.; Olmstead, M. M. *J. Am. Chem. Soc.* **1990**, *112*, 5181.
(24) Klabunde, U. *Inorg. Synth.* **1974**, *15*, 82.
(25) Ray, P. C.; Sen, S. C. *J. Indian Chem. Soc.* **1930**, *7*, 67.
(26) Appel, R.; Geisler, K.; Scholer, M.-F. *Chem. Ber.* **1979**, *112*, 648.
(27) *International Tables for X-ray Crystallography*; Kynoch Press: Birmingham, England, 1974; Vol. 14.
(28) The method obtains an empirical absorption tensor from an expression relating F_o and F_c: Moezzi, B. Ph. D. Thesis, University of California, Davis, 1987.

only random variations in intensity during data collection.

Calculations were performed as described above on data that had been corrected for Lorentz and polarization effects. Iridium and gold heavy atom positions were determined via Patterson methods. All non-carbon atoms of the cation along with the carbonyl carbon, C(1), were refined with anisotropic thermal parameters, while all others were refined with isotropic thermal parameters. All phenyl rings were modeled as rigid groups. Bond lengths and angles were also fixed for the hexafluorophosphate ion. The hydrogen atom positions on methylene carbons were included by using a riding model with a C-H vector fixed at 0.96 Å and a thermal parameter 1.2 times the host carbon. An absorption correction was applied.[22] The largest peak in the final difference map had density equal to 7.0 electrons/Å^3. This peak is 0.991 Å from Au(1).

$[Ir(CN)_2Au_2(\mu\text{-dpmp})_2][PF_6]$. Dichroic purple/gold crystals were obtained with difficulty by slow diffusion of toluene into a dichloromethane solution of the complex. The crystal was handled as described above. Unit cell parameters were determined by least-squares refinement of 11 reflections with $16 < 2\theta < 23°$. Two check reflections exhibited only random (<2%) variation during data collection. Crystal data are given in Table IV.

Calculations were performed as previously outlined. Iridium and gold heavy atom positions were determined from a Patterson map with the iridium positioned on the inversion center. All non-carbon atoms of the cation along with the cyanide carbon, C(1), were refined with anisotropic thermal parameters, while all others were refined with isotropic thermal parameters. The hydrogen atom positions were calculated by using a riding model with a C-H vector fixed at 0.096 Å and a thermal parameter 1.2 times the host carbon. An absorption correction was applied.[28]

There are two toluene molecules in the crystal lattice. One of these is disordered. For the latter, atomic positions are shared for six phenyl carbon atoms, while the methyl group is disordered between two para positions. A dichloromethane molecule is also present in the lattice at 25% occupancy. The largest unassigned peak in the final difference map had density equal to 8.3 electrons/Å^3. This peak is 0.571 Å from Ir(1). A 3 electrons/Å^3 peak is located at (0.5, 0.5, 0) but represents an unreasonable contact with the PF_6^- anion. The goodness of fit was calculated at 1.477.

Acknowledgment. We thank the National Science Foundation (Grant CHE 894209) for support, Johnson Matthey, Inc. for a loan of gold and iridium salts, and Professor Peter B. Kelly for experimental assistance.

Supplementary Material Available: Tables of atomic coordinates, bond distances, angles, anisotropic thermal parameters, hydrogen atom positions, and refinement data for **4**, **6**, and **7** (22 pages); tables of observed and calculated structure factors (102 pages). Ordering information is given on any current masthead page.

Reactions of Aryl-Iron(III) Porphyrins with Dioxygen. Formation of Aryloxy-Iron(III) and Aryl-Iron(IV) Complexes

Ramesh D. Arasasingham,[†] Alan L. Balch,*[†] Rebecca L. Hart,[†] and Lechosław Latos-Grażyński[‡]

Contribution from the Departments of Chemistry, University of California, Davis, California 95616, and the University of Wrocław, Wrocław, Poland. *Received December 1, 1989*

Abstract: The reaction of dioxygen with low-spin, five-coordinate complexes, $PFe^{III}Ar$ (P, porphyrin dianion; Ar, aryl group) has been examined for comparison with previous work (Arasasingham, R. D. et al. *J. Am. Chem. Soc.* **1989**, *111*, 4357) on the corresponding alkyl complexes which showed that peroxo complexes $PFe^{III}OOR$ formed initially and then decomposed to form PFeOH and an aldehyde or ketone when R was a primary or secondary alkyl group. Dioxygen addition to $TTPFe^{III}(C_6H_4CH_3\text{-}p)$ at 25 °C in toluene yields the phenoxide complex, $TTPFe(OC_6H_4CH_3\text{-}p)$, as the principle product, while addition to $TTPFe^{III}C_6H_5$ at -30 °C yields $TTPFe^{III}OC_6H_5$ and small amounts of $TTPFe^{III}(OC_6H_4OH\text{-}p)$ and $TTPFe^{III}OC_6H_4OFe^{III}TTP$. These reactions have been monitored by both ^1H NMR and ESR spectroscopies. No intermediates have been detected in the formation of these products. Mechanisms for the formation of these products have been formulated in terms of the initial insertion of dioxygen into the Fe-C bond followed by rapid homolysis to form $PFe^{IV}{=}O$ and $^{\bullet}OAr$, with subsequent reactions yielding the final products. Addition of dioxygen to a solution of $TTPFe^{III}(C_6H_4CH_3\text{-}p)$ in chloroform at -60 °C yields a mixture of $[TTPFe^{IV}(C_6H_4CH_3\text{-}p)]^+$ and $TTPFe^{III}Cl$ with no evidence for the formation of the phenoxide complexes. In this case electron transfer to yield the oxidized iron porphyrin and superoxide ion is driven by the solvent polarity and the ability of the solvent to destroy superoxide ion as it is formed.

Introduction

The inactivation of hemoglobin and myoglobin by arylhydrazines in the presence of dioxygen leads to the formation of green pigments which have been identified as *N*-phenylheme.[1-3] Spectroscopic and chemical studies,[3-5] including X-ray structural analysis on the myoglobin complex,[6] have unambiguously demonstrated that phenyl-iron(III) porphyrins are key intermediates in this process. Studies on natural hemeproteins and on model systems have demonstrated that the phenyl group migrates from the iron to the nitrogen under oxidizing conditions.[2-10] Electrochemical and optical spectroscopic studies have suggested that this process occurs via several intermediates as shown in Scheme I.

Scheme I

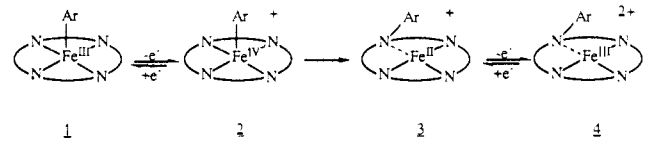

1 2 3 4

[†] University of California, Davis.

[‡] University of Wrocław.

[§] Abbreviations used: P, porphyrin dianion; TTP, tetra-*p*-tolylporphyrin dianion; TMP, tetramesitylporphyrin dianion; OEP, octaethylporphyrin dianion; Ar, generic aryl group.

(1) Saito, S.; Itano, H. A. *Proc. Natl. Acad. Sci.* U.S.A. **1981**, *78*, 5508.
(2) Ortiz de Montellano, P. R.; Kunze, K. L. *J. Am. Chem. Soc.* **1981**, *103*, 6534.
(3) Augusto, O.; Kunze, K. L.; Ortiz de Montellano, P. R. *J. Biol. Chem.* **1982**, *257*, 6231.
(4) Kunze, K. L.; Ortiz de Montellano, P. R. *J. Am. Chem. Soc.* **1983**, *105*, 1380.

0002-7863/90/1512-7566$02.50/0